Available online www.jsaer.com

***Journal of Scientific and Engineering Research*, 2017, 4(5):86-93**

Research Article

ISSN: 2394-2630
CODEN(USA): JSERBR

Investigation of Tectonic Structure of Turkey-Hatay Region Using Markov Random Fields (MRF)

Ali Muhittin ALBORA

Istanbul University, Engineering Faculty, Geophysical Department, 34320, Avcilar, Istanbul, Turkey

Abstract The most important topics of gravity and magnetic anomaly maps from geophysical studies are interpreted best by separating the regional structure and the residual structure. In this study, Markov Random Fields (MRF) method was used for this purpose to distinguish between regional and residual fields. We present a dynamic programming based on evaluation of noisy and super positioned effects of the various geological structures considering a statistical maximum a posteriori (MAP) criterion. The objective of the proposed modelling is to capture the intrinsic character of the input potential field anomaly map in a few parameters to understand the nature of the phenomenon generating the anomaly. In this study, gravity anomaly map of the input data is considered as a 2-dimensional image with a matrix com-posed of N1xN2 pixels. We evaluate each pixel of N1xN2 matrix using MRF approach, with respect to the neighbouring pixels and locality of their connections in real time with no priori processing. The most important feature of the MRF method is that it does not require preliminary training and utilization of the stochastic properties of the neighbourhood and two-dimensional view. In order to prove the success of this method, a synthetic study was carried out on the prisms and very good results were obtained. The gravity anomaly map of the Turkey-Hatay region was used as a land study. The tectonic lines of the Turkey-Hatay region have been revealed at the end of the MRF outputs.

Keywords Markov Random Fields (MRF), Turkey-Hatay region, Tectonic lines

Introduction

One of the most important factors in the interpretation of gravity and magnetic anomaly maps is to remove from unwanted noise. In other words, the most important problem is the separation of near-surface structures (residual) and deeply localized (regional) effects. If the removal of residual anomaly maps is desired, the regional effects are undesirable for us. Considering this situation, it is necessary to use filter techniques according to the searched structures. Another important factor in interpreting the maps of potential sources is the determination of discontinuity boundaries. For this reason, the Markov Random Fields (MRF) method has been used both as a separation method and as a structure limit analysis in this study. In order to test the success of the method in synthetic areas, a model structure consisting of prismatic structures was used in the coordinates at different depths. The MRF method has shown successful results in the model study. The gravity anomaly map of Hatay region was used as land application. The most important feature of the MRF method is that it utilizes the stochastic structure of neighbouring relations and two-dimensional view. Moreover, the MRF method does not require preliminary training and therefore our data loss is reduced. Implemented the first application of the MRF approach to two-dimensional images [1-4]. Since Turkey is located on active tectonic lines, many effective earthquakes occur. The North Anatolian Fault Zone (NAFZ) in the North and the Eastern Anatolian Fault Zone (DAFZ) in the East are active faults and these fault lines constitute too many large earthquakes. Hatay region is one of our illnesses where seismic activity is high. Although the gravity anomaly has important effects on some faults in the Hatay region, the effect of the Dead Sea Fault (DSF), which is one of the important

strike-slip faults of the region, cannot be observed sufficiently. The MRF method was applied to the Bouguer anomaly map in order to make the gravity effects of the faults existing in Hatay region more prominent. Thus, the structure boundary map was determined and the tectonic map of the region was updated. The area is an important place of tectonic agony. For this reason, many scientists are discussing the tectonics of the region [5-6].

Materials and Methods: Markov Random Field (MRF) Approach

The stochastic models depending on MRF approach in 2-D data analysis has led to the development of many practical algorithms that would not have been realized with *ad-hoc* processing [1-4]. A random field is a joint distribution imposed on a set of random variables representing objects of interest, such as pixel intensities, that imposes the statistical dependence in a spatially meaningful way. Gravity anomaly map, we investigate is assumed to be a finite $N_1 X N_2$ rectangular *lattice* of points (pixels) defined as. The application of MRA has been made to detect discontinuity boundaries and $x = \{xij\}$.The X random variable is called $Q = \{q_1, q_2, q_3, ...q_M\}$ and M is one of the values. The transition from the Y anomaly map to the X residual map is in accordance with Bayes' rule and the probability of transition is $P(X=x/Y=y)$.

$$P(X = x / Y = y) = \frac{P(Y = y|X = x)P(X = x)}{P(Y = y)} \quad (1)$$

Since probability, $P(Y=y)$ does not affect maximization, logarithmic of Equation (1) can be written as,

$$\ln P(X=x,Y=y) = \ln P(X=x) + \ln P(X=x/Y=y) \quad (2)$$

Equations 3 and 4 are obtained by performing a number of operations on Equation 2.

$$\ln P(X = x) = -\ln Z - \sum_{c \in C} V_c(x) \quad (3)$$

$$\ln P(Y = y|X = x) = -\frac{N_1 N_2}{2} \ln(2\pi\sigma^2) - \sum_{m=1}^{M} \sum_{(i,j) \in S_m} \frac{1}{2\sigma^2} (s_{ij} - q'_m)^2 \quad (4)$$

where, $S_m = \{(i, j) \in L : X_{ij} = m\}$. Z is defined, q_m' is the transient quantization level of residual map during optimization and $V_c(x)$ is the potential associated with clique c [7-8]. Consider a site (i,j) and its neighbourhood η_{ij} at residual map of X. Let q_m' is the transient quantization level of residual map during optimization at (i,j) pixel and t' represent the vector of neighbouring values of q_m' at (i,j) (Figure 1).

V_1	U_2	V_2
U_1	q_m'	U_3
V_3	U_4	V_4

Figure 1: Q_m' and η_{ij} of residual magnetic map.

$$t' = [u_1, u_2, u_3, u_4, v_1, v_2, v_3, v_4]^T \quad (5)$$

Here t' neighbourhoods are given. If the intermediate operations are skipped, the right side of equation (3) can be written as,

$$V(q'_m, t', \theta) \equiv \sum_{c: q'_m \in C} V_C(x) \quad (6)$$

where Θ is the parameter vector. Θ is defined as,

$$\theta = [\alpha_1, \alpha_2, .., \alpha_M, \beta_1, \beta_2, \beta_3, \beta_4, \gamma_1, \gamma_2, \gamma_3, \gamma_4, \xi_1]^T \quad (7)$$

Then we can rewrite (6) as,

$$V(q_m^{'}, t', \theta) \equiv \phi^T(q_m^{'}, t')\theta \quad (8)$$

where,

$$\phi(q_m^{'}, t') = [J_1(q_m^{'}), J_2(q_m^{'}), ..., J_M(q_m^{'}), (I(q_m^{'}, u_1) + I(q_m^{'}, u_3)), (I(q_m^{'}, u_2) + I(q_m^{'}, u_4)),$$
$$(I(q_m^{'}, v_2) + I(q_m^{'}, v_4)), (I(q_m^{'}, v_1) + I(q_m^{'}, v_3)), (I(q_m^{'}, u_2, v_2) + I(q_m^{'}, u_4, u_3) + I(q_m^{'}, u_1 v_4)),$$
$$(I(q_m^{'}, u_4, v_3) + I(q_m^{'}, u_2, u_3) + I(q_m^{'}, u_1, v_1)), (I(q_m^{'}, u_2, v_1) + I(q_m^{'}, u_1, u_4) + I(q_m^{'}, u_3, v_3)),$$
$$(I(q_m^{'}, u_1, u_2) + I(q_m^{'}, u_4, v_4) + I(q_m^{'}, u_3, v_2)), (I(q_m^{'}, u_1, v_1, u_2) + I(q_m^{'}, u_2, v_2, u_3) +$$
$$I(q_m^{'}, u_3, v_3, u_4) + I(q_m^{'}, u_4, v_4, u_1))]^T \quad (9)$$

Here *I* and *J* are indicator functions. Thus, MRA was obtained.

Application of MRF methods to synthetic applications

Table 1: Parameters of prisms with different sizes

Parameters	prism 1	prism 2	Prism 3
(x,y) coordinates	(31,31)	(39,40)	(20,37)
h (depth)	50	6	5
r (radius)	30	4	4
ρ (density)	1.5	1.2	1

As a synthetic study, the Bouguer anomaly map brought up by 3 different sphere anomalies was discussed. Here, two spheres are close to the surface and have a residual effect and 3 spheres are deep and have regional effect. The parameters of these spheres with different parameters are shown in Table 2. In both studies, the success of the MRF method in distinguishing between regional and residual anomalies has yielded quite good results (Figure 2).

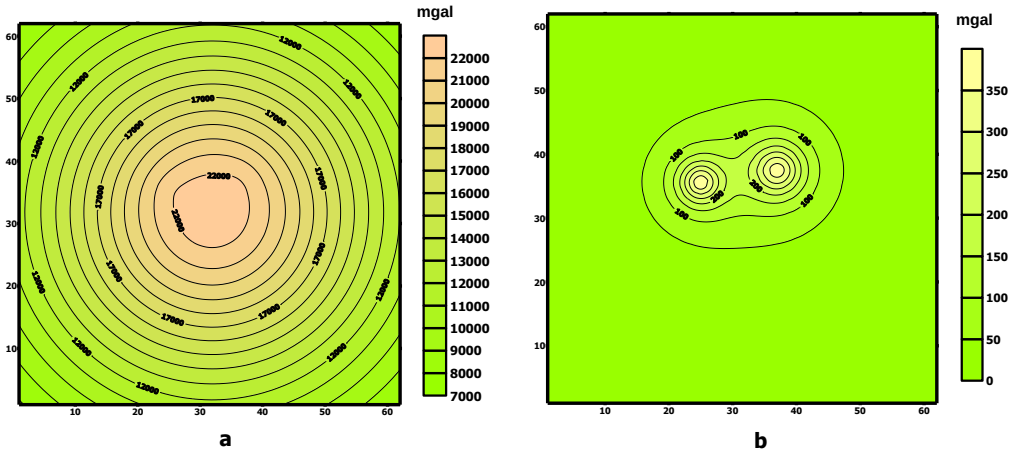

Figure 2: Three prisms with different parameters a) Bouguer anomaly map b) MRF output of Bouguer anomaly map.

Application of MRF method to Hatay Region Bouguer Anomaly Map

When the Bouguer anomaly map is examined (Figure 3), -35 mgal contour values are observed especially towards the east. In the western part of the Bouguer anomaly, an anomaly of up to 80 mgal is observed, especially on the Amanos Mountains. The Bouguer gravity anomaly map shown in Figure 3 cannot be clearly seen because the Dead Sea Fault (DSF) is covered with a young alluvial cover. However, the effects of the fault on the western side of this fault seem more obvious. The MRF method was applied to the Bouguer anomaly map to reveal and trace the gravity anomalies caused by the tectonic structure (Figure 4).

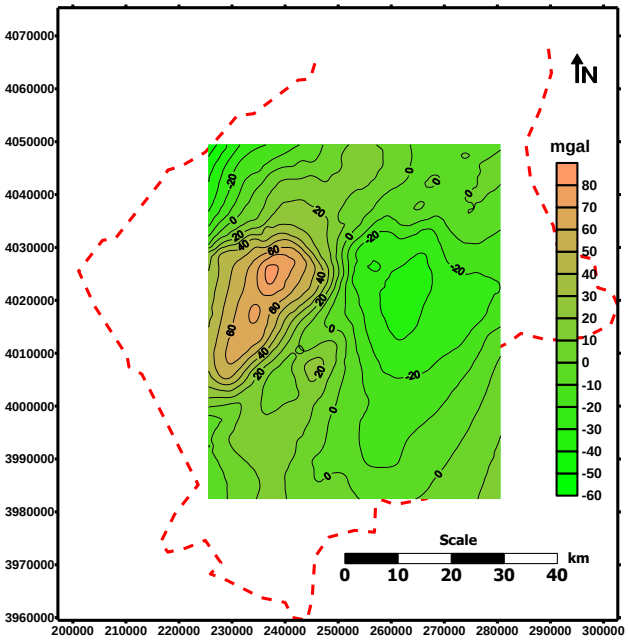

Figure 3: Map of Bouguer anomaly map of Hatay region.

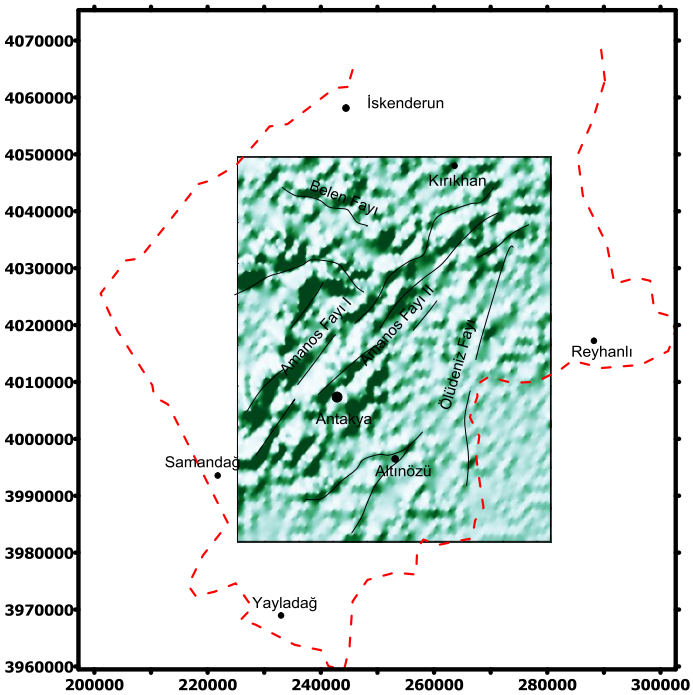

Figure 4: Hatay region the output of the Bouguer anomaly map after applying MRF (Black straight lines show the locations of the fault lines in the region)

Geology and Tectonic Structure of Hatay

In Hatay Region, young tectonic movements have formed Amanos Mount, Iskenderun Bay and Hatay graben. In the South of Amanos Mountains, a continuous ophiolite succession, the Kizildag ophiolite, is exposed from tectonism peridotites, through layered and isotropic gabbros to the sheeted dike complex and pillowed volcanic[9,10]. Here, the young tectonic movements are taken into consideration, starting from Arabia to North-North East and Anatolian block movements to West. Dead Sea Fault (DSF) zone is a tectonic structure with 1000 km in length starting from Dead Sea and ending at Hatay [11-14]. DSF, starting from Maras, tending to South-North to Dead Sea, is the main fault system forming Hatay graben. It is assumed that DSF is formed as a rift of Arabian plate and Africa plate and their rotation to North with counter clockwise of 6-7 degrees [15-19]. Estimated the slip rate on the Arava segment of the Dead Sea Fault Zone (DSFZ) as 4 ± 2 mm a^{-1}. Predicted the slip rate, as slip rate on the southern DSF is 4 mm a^{-1} using DSF geology and GPS data [20].

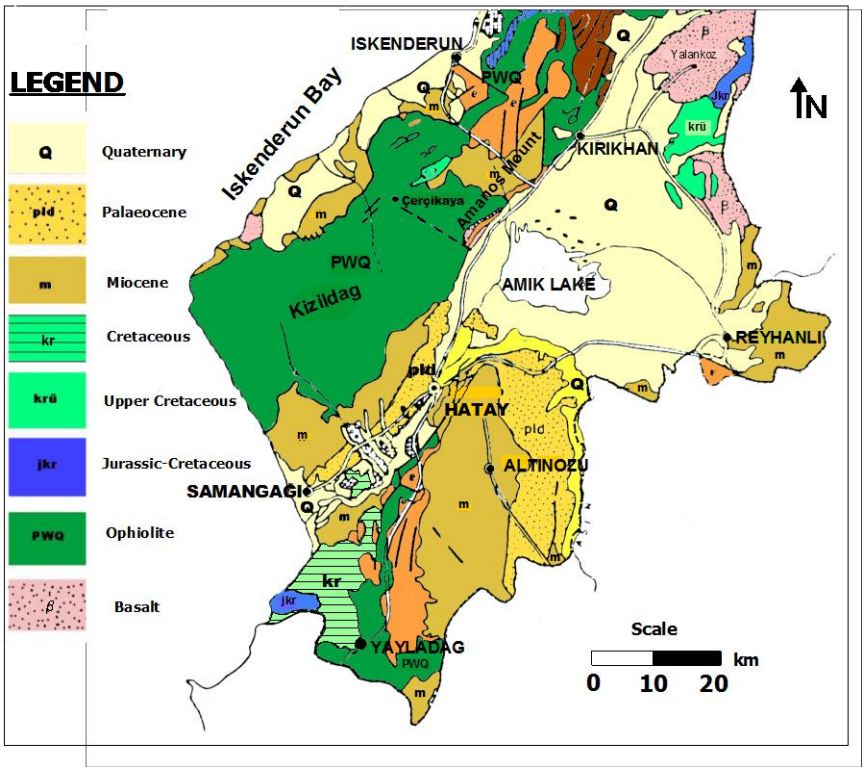

Figure 5: Geological map Hatay (The original map is obtained from Technical Ore Research of Turkey (MTA)).

This displacement has resulted left lateral faults from South to North. In Hatay, Amik area is Pliyo-Kuvaterner with 30 km length [18, 21]. The force forming the fault has also affected the sedimentary rocks, which lie on the West and East of the fault with 90 degrees angle [22]. DSF is more effective in Syria than in Turkey since Amik plane composed of alluvial in Turkey covers it [5]. West graben fault is the region of Kahramanmaraş and Kırikhan and surrounded by East of Amonos Mountains and vertical shift is dominant (Figure 5). Erzin–Iskenderun fault, which makes Amanos Mountains to be seen as horst forms district faults in Iskenderun basin [6, 23-25].

Earthquake Activity

Geological and kinematic determinations of the North Anatolian Fault Zone (KAFZ) and their lateral, sinistral shifts [26, 27]. There are two earthquakes greater than 7 in Hatay Region. These are: 13 August 1822 and 3 April 1872 [28]. These earthquakes are shown in stars in Figure 6. The magnitudes greater than 5 are shown in blank squares and the ones greater than 4 are in dark circles as in Figure 6. The data are obtained from USGS, ISC and Kandilli Research Canter. Most of the earthquakes result as a shift of Anatolian block by African-

Arabian plates. These activities are occurred along the active faults. The focal mechanisms of shallow earthquakes occurred along the Hatay region is given in Table 2.

Table 2: Parameters of focal mechanisms of shallow earthquakes occurred along the Hatay region [29-31].

Loc. No	Date	Latitude	Longitud	Plane 1 direc^0/slope^0	Plane 1 direc^0/slope^0	T-axis Az/dip	Magnit. M_b	Dip (km)
1	01.01.1975	36.67	36.49	300/65	198/44	58/14	4.8	35
2	24.06.1989	36.28	36.13	203/28	27/62	115/17	5.1	15
3	22.01.1997	36.23	35.85	208/38	331/68	80/17	5.5	33
4	22.01.1997	36.21	35.65	228/42NW	358/62	108/10	5.2	33
5	22.01.1997	39.21	35.92	225/43	355/64	108/10	5.3	33

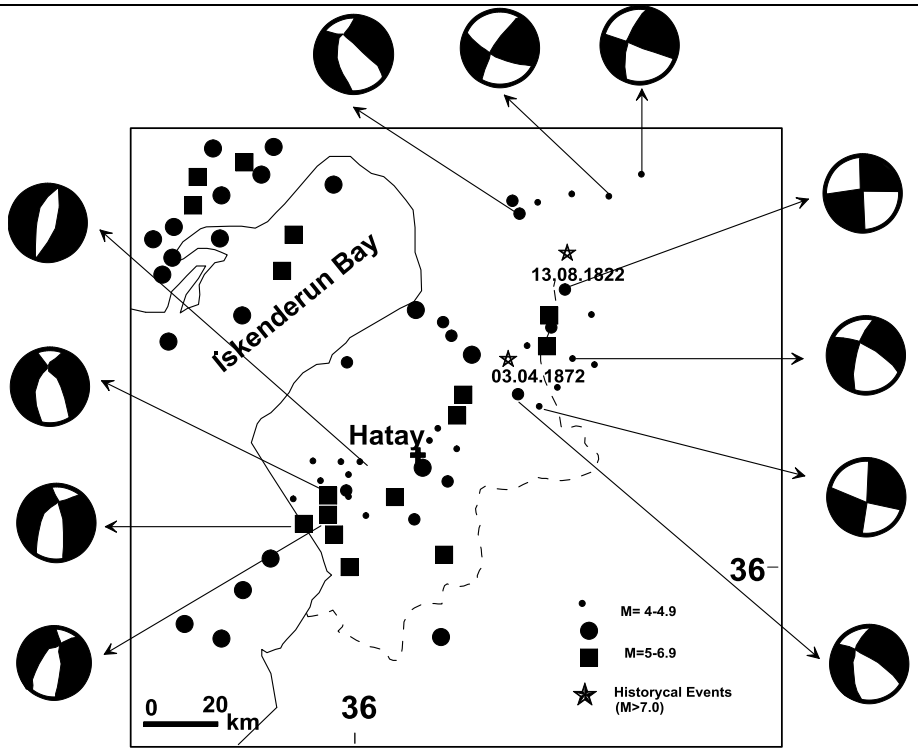

Figure 6: Seismotectonic features of Hatay region (modified form of Over et al., 2004).

Conclusion

The effect of structures not visible in the Bouguer gravity anomaly was evident in the results obtained after the MRF method was applied. When the tectonic structure of the region is revealed, the MRF output and the geology related data of the region should be evaluated together. For example, the DSF is covered with young alluvium, so it is not seen in topography, surface geology and gravity anomalies. The effect of the fault appears after the MRF method is applied to the Bouguer anomaly map. All the results were evaluated together and a map showing the tectonic structure of the region was prepared (Figure 7). Two large tectonic units have been distinguished on the map. The prepared tectonic map is distinguished by an old tectonic structure which can be described as a reverse fault. The Belen fault, which is also seen from geological maps, is also clearly seen in the map prepared in this study. As a result, the tectonic map of the region was prepared by evaluating the map of Bouguer gravity anomaly and the results of the MRF method. The prepared map appeared in accordance with the geology of the region.

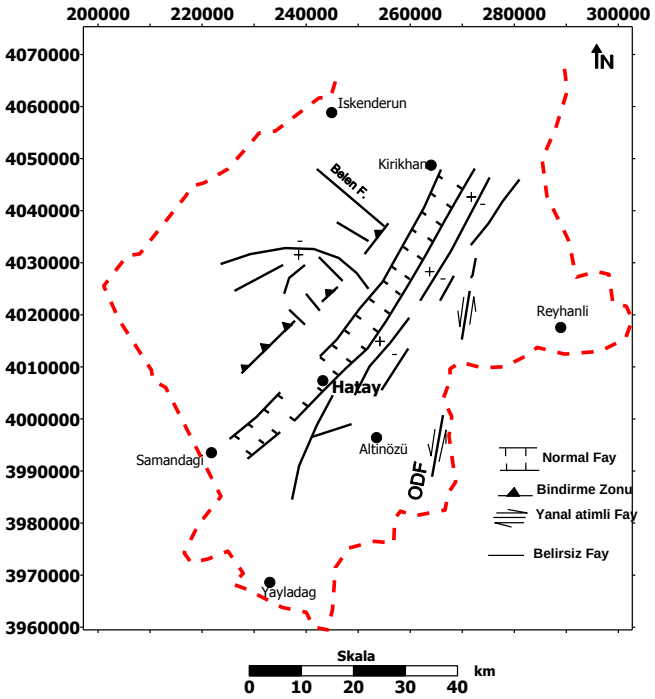

Figure 7: New tectonic map of Hatay region

Contributions

We thank Turkish Petroleum Cooperation (TPAO) and for their gravity data. We are also grateful to Technical Ore Research of Turkey (MTA) for their geological map.

References

[1]. Geman, S., & Geman, D. (1984). Stochastic Relaxation, Gibbs Distributions, and the Bayesian restoration of images, *IEEE PAMI*, 6:721-741.

[2]. Derın, H., & Ellıot, A.H., (1987). Modelling ans segmentation of noisy and textured images using Gibbs Random Field, *IEEE PAMI*, 9: 39-55.

[3]. Dubes, R.C., & Jain, A. (1989). Random field models in image analysis, *Journal of Applied Statistics*, 16:131-162.

[4]. Uçan, O.N., Şen, B., Albora, A.M., & Özmen, A. (2000). A New Gravity Anomaly Separation Approach: Differential Markov Random Field (DMRF), *Electronic Geosciences*, 5(1):1-7.

[5]. Albora, A.M. (1998). Investigation of gravity density distribution in Hatay region (in Turkish). *Ph. D. Thesis*, Istanbul Univ., Science Inst., Istanbul.

[6]. Demirel, S. (1993). Evaluation of the geophysical data on İskenderun Bay (in Turkish), *Ph. D. Thesis*, Istanbul Univ., Science Inst., Istanbul.

[7]. Ising, E. (1925). *Zeitschrift Physik*, 31, 253.

[8]. Uçan, O.N., & Albora, A. M. (2009). Evaluation of Ruins of Hittite Empire in Sivas-Kusakli Region Using Markov Random Field (MRF), *Near Surface Geophysics*, 7(2):111-122.

[9]. Coleman, R. G. (1981). Tectonic setting of ophiolite obduction in Oman, *Jour. Geophys. Res.*, 86: 2497-2508.

[10]. Tekeli, O., & Erendil, M. (1986). Geology and petrology of the Kizildag ophiolite (Hatay). *Bulletin of the Mineral Research and Eploration*, 107: 21-38.

[11]. Nur, A., & Ben-Avraham Z., (1978). The eastern Mediterranean the Levant: Tectonics of continental collision. *Tectonic*, 46:297-311.

[12]. Lovelock, P, E, R., (1984). A review of the tectonics of the northern Middle-East region. *Geological Magazine*, 121: 577-587.

[13]. Hempton, M. R., (1987).Constraints on Arabian plate motions; an extensional history of the Red sea. *Tectonics*, 6: 668-705.

[14]. Ambraseys, N. N., & Barazangi, M., (1989). The 1795 earthquake in the Bekaa Valley: Implications for earthquake hazard assessment in the eastern Mediterranean region. *J. Geophys. Res*. 94: 4007-4013.

[15]. Mc Kenzie, D. P., (1972). Active tectonics of the Mediterranean Region. *Geophs. J. R. Astron. Soc.* 30: 109-185.

[16]. Mc Kenzie, D. P., (1978). Active tectonics of the Alpine-Himalayan belt: the Aegean Sea and surrounding regions (tectonics of Aegean region). *Geophs. J. R. Astron. Soc*., 55: 217-254.

[17]. Jackson, J. A. & Mc Kenzie, D. P., (1988).Active tectonics of the Alpine-Himalayan belt between western Turkey and Pakistan. *Geophs. J. R. Astron. Soc*., 93:45-73.

[18]. Lybéris N., Yurur, T., Chorowicz, J., Kasapoglu, K.E. & Gundogdu, N., (1992). The East Anatolian Fault: an oblique collisional belt. *Tectonophysics*. 204: 1-15.

[19]. Hisarlı, Z.M., Albora, A.M. & Uçan, O.N., (2001). The interpretation of tectonic structure of the region using Gravity anomaly map of Hatay region. *14. Geophysical Congress (MTA)-ANKARA*, 162-167.

[20]. Klinger, Y., Avouac, J. P., Abou, K. N., Dorbath, L., Bourles, D., & Reyss, J. L., (2000). Slip rate on the Dead Sea transform fault in northern Arava Valley (Jordan). *Geophys. J. Int.*, 142:755-768.

[21]. Westaway, R., (2003). Kinematics of the Middle East and Eastern Mediterranean Updated. *Turkish J. Earth Sci.*, 12: 5-46.

[22]. Perinçek D., & Cemen, I., (1990). The structural relationship between the East Anatolian Fault and Dead Sea Fault zones in southern Turkey. *Tectonophysics*. 172: 331-340.

[23]. Alp H., Albora A.M., &Tur H., (2011). A View of Tectonic Structure and Gravity Anomalies of Hatay Region Southern Turkey Using Wavelet Analysis. *Journal of Applied Geophysics*, 75:498-505.

[24]. Alp, H., & Albora, A.M., (2006). Monitoring of Eastern Anatolian Fault by using wavelet analysis method. *Active Tectonic Researces Group 10th Meeeting ATAG10*. 2-4.

[25]. Alp, H. & Albora, A.M.,(2007). A look East Anatolian Fault using wavelet analysis method. *e-Journal of New World Sciences Academy*, 2, (3): 232-240.

[26]. Eyidogan, H., (1983). Seismotectonic properties of the Bitlis-Zagros thrust belt (in Turkish). *PhD thesis*, Istanbul Tech. Univ. Fac. Minning, Istanbul

[27]. Taymaz, T., Eyidoğan, H., &Jackson, J.,(1991). Source parameters of large earthquakes in the East Anatolian Fault Zone (Turkey). *Geophys. J. Int.* 106: 537-550.

[28]. Ambraseys, N. N., & Barazangi, M., (1989). The 1795 earthquake in the Bekaa Valley: Implications for earthquake hazard assessment in the eastern Mediterranean region. *J. Geophys. Res.*, 94: 4007-4013.

[29]. Buyukasıkolu, S., (1980). Characteristics of the Eurasian-African plate nerve in the northern and southern Anatolia of the Eastern Mediterranean gyre. *Earthquake Research Bulletin* (in Turkish). 29: 58-74.

[30]. Erdik M., Aydinoglu, N., Pinar, A., & Kalafat, D. (1997). *Hatay Earthquake Report*. Kandilli Rasahanesi Recordings Istanbul.

[31]. Over, S., Unlugenc, U. C., & Ozden, S. (2001). The stress states acting in the Hatay region. *Bulletin Earth Sciences Application and Research Centre of Hacettepe University*. 23:1-14.